Physics Letters B 706 (2011) 6–12

Contents lists available at SciVerse ScienceDirect

Physics Letters B

www.elsevier.com/locate/physletb

W/Z bremsstrahlung as the dominant annihilation channel for dark matter, revisited

Nicole F. Bell [a], James B. Dent [b], Ahmad J. Galea [a], Thomas D. Jacques [a], Lawrence M. Krauss [b,c], Thomas J. Weiler [d,*]

[a] School of Physics, The University of Melbourne, Victoria 3010, Australia
[b] Department of Physics and School of Earth and Space Exploration, Arizona State University, Tempe, AZ 85287-1404, USA
[c] Research School of Astronomy and Astrophysics, Australian National University, Canberra, Australia
[d] Department of Physics and Astronomy, Vanderbilt University, Nashville, TN 37235, USA

ARTICLE INFO

Article history:
Received 19 October 2011
Accepted 24 October 2011
Available online 25 October 2011
Editor: S. Dodelson

Keywords:
Dark matter annihilation

ABSTRACT

We revisit the calculation of electroweak bremsstrahlung contributions to dark matter annihilation. Dark matter annihilation to leptons is necessarily accompanied by electroweak radiative corrections, in which a W or Z boson is also radiated. Significantly, while many dark matter models feature a helicity suppressed annihilation rate to fermions, bremsstrahlung process can remove this helicity suppression such that the branching ratios $\mathrm{Br}(\ell\nu W)$, $\mathrm{Br}(\ell^+\ell^- Z)$, and $\mathrm{Br}(\bar{\nu}\nu Z)$ dominate over $\mathrm{Br}(\ell^+\ell^-)$ and $\mathrm{Br}(\bar{\nu}\nu)$. We find this is most significant in the limit where the dark matter mass is nearly degenerate with the mass of the boson which mediates the annihilation process. Electroweak bremsstrahlung has important phenomenological consequences both for the magnitude of the total dark matter annihilation cross section and for the character of the astrophysical signals for indirect detection. Given that the W and Z gauge bosons decay dominantly via hadronic channels, it is impossible to produce final state leptons without accompanying protons, antiprotons, and gamma rays.

1. Introduction

The importance of electroweak radiative corrections to dark matter annihilation has recently been recognized, and examined in a number of publications [1–10]. In a recent paper some of the present authors considered electroweak bremsstrahlung contributions to dark matter annihilation, in models in which dark matter annihilation to a fermion–antifermion pair, $\chi\chi \to \bar{f} f$, is helicity suppressed [1]. There it was shown that W/Z bremsstrahlung lifts helicity suppressions, and can therefore be the dominant DM annihilation mode. However, some of the quantitative conclusions of [1] must be modified, as the explicit cross section calculation therein was in error.[1] The purpose of the present Letter is to revisit and extend the calculation of the W/Z bremsstrahlung cross sections, and draw inferences from the result. The main inference is that the three body final state processes can still dominate the tree level process as claimed in [1]. We show herein that the claim finds support in the region where the parameter $\mu \equiv m_\eta^2/m_\chi^2$ is not too far from unity, with m_η and m_χ being the mass of the boson which mediates the annihilation process and the dark matter mass, respectively. This region of parameter space is reminiscent of the co-annihilation region in standard supersymmetric (SUSY) scenarios, although the present work can also be applied to models which are not in the SUSY framework.

Let us parametrize the dark matter annihilation cross section in the usual way,

$$\sigma v = a + b v^2, \tag{1}$$

where the constant a arises from s-wave annihilation while the constant b receives contributions from both s- and p-wave channels. Since the dark matter velocity in a galactic halo today is $v \sim 10^{-3}c$, the p-wave term is strongly velocity suppressed. In order to have a large annihilation cross section in the Universe today, it is desirable to have an unsuppressed a (s-wave) term. However,

* Corresponding author.
E-mail address: t.weiler@vanderbilt.edu (T.J. Weiler).

[1] The generalized Fierz identities derived and presented in this paper (main text and Appendix A) are all correct. However, due to parallel processing of our efforts, our explicit cross section calculation was performed using an incorrect Fierz identity from the textbook by Okun [11]. In the notation of Ref. [11] this identity should read $F_l^i G_k^m = \frac{1}{4}\sum_A \Delta_A (F\gamma_A G)_l^m (\gamma_A)_k^i$, but does not, with indices incorrectly interchanged, equivalent to exchanging F and G on one side of the equation. Accordingly, we obtained incorrect cross-section results. In fact, we now find that the s-wave contributions to the bremsstrahlung cross sections cancel exactly in the four Fermi limit (the subject of Ref. [1]). The non-zero results of the present Letter are obtained at one order higher in the inverse of the propagator mass, $1/m_\eta^2$.

0370-2693/$ – see front matter
doi:10.1016/j.physletb.2011.10.057

the s-wave annihilation of DM to a fermion–antifermion pair is helicity suppressed in a number of important and popular models. The most well known example is the annihilation of supersymmetric neutralinos to a fermion–antifermion pair. The circumstances under which helicity suppressions do or do not arise were discussed in detail in Ref. [1].

It has long been know that bremsstrahlung of photons can lift such a helicity suppression, leading to the result that the cross section for $\chi\chi \to \bar{f} f \gamma$ can dominate over that for $\chi\chi \to \bar{f} f$ [12–17]. However, the fact that radiation of a W or Z gauge boson would also lift a helicity suppression had been overlooked until the work of Refs. [1,4]. In these scenarios for which the helicity suppression is removed, the dominant annihilation channels are the set of bremsstralung processes, namely γ, W and Z bremsstrahlung. (If the dark matter annihilates to colored fermions, radiation of gluons would also contribute.) The phenomenology of W and Z bremsstrahlung is richer than that for photon bremsstrahlung alone. This is because the W and Z bosons decay dominantly to hadronic final states, including antiprotons, for which interesting cosmic ray bounds exist.

2. Example of suppressed annihilation

To illustrate our arguments, we choose a simple example of the class of model under discussion. This is provided by the leptophilic model proposed in Refs. [18,19]. Here the DM consists of a gauge-singlet Majorana fermion χ which annihilates to leptons via the $SU(2)$-invariant interaction term

$$f\left(\nu\ell^-\right)_L \varepsilon \begin{pmatrix}\eta^+\\ \eta^0\end{pmatrix}\chi + \text{h.c.} = f\left(\nu_L\eta^0 - \ell_L^-\eta^+\right)\chi + \text{h.c.} \tag{2}$$

where f is a coupling constant, ε is the 2×2 antisymmetric matrix, and (η^+, η^0) is a new $SU(2)$ doublet scalar. In this model, DM annihilation to fermions is mediated by t and u channel exchange of the η fields.

An identical coupling occurs in supersymmetry if we identify χ with a neutralino and η with a sfermion doublet. In fact, the implementation of supersymmetric photinos as dark matter by H. Goldberg provided the first explicit calculation of s-wave suppressed Majorana dark matter annihilation to a fermion pair [20]. Therefore, much of what we discuss below is also relevant for neutralino annihilation to fermions via the exchange of sfermions. However, the class of models for which the $2\to 2$ annihilation is helicity suppressed is more general than the class of supersymmetric models.

The cross section for the $2\to 2$ process $\chi\chi \to e^+e^-$ or $\nu\bar{\nu}$ is given by

$$v\sigma = \frac{f^4 v^2}{24\pi m_\chi^2}\frac{1+\mu^2}{(1+\mu)^4}, \tag{3}$$

where $m_l \simeq 0$ and $m_{\eta^\pm} = m_{\eta^0}$ have been assumed, and $\mu = m_\eta^2/m_\chi^2$. The suppressions discussed above are apparent in Eq. (3). The helicity suppressed s-wave term is absent in the $m_l = 0$ limit, and thus only the v^2-suppressed term remains.

3. Lifting the suppression with electroweak bremsstrahlung

3.1. W-strahlung cross section

We shall take the limit $m_l \simeq 0$ and assume that $m_{\eta^\pm} = m_{\eta^0}$. The matrix elements for the six diagrams of Fig. 1 are given by

$$\mathcal{M}_a = i\frac{f^2 g}{\sqrt{2}}\frac{1}{q_1^2}\frac{1}{t_1 - m_\eta^2} \times \left(\bar{v}(k_2)P_L v(p_2)\right)\left(\bar{u}(p_1)\gamma^\mu P_L \not{q}_1 u(k_1)\right)\epsilon_\mu^Q, \tag{4}$$

$$\mathcal{M}_b = i\frac{f^2 g}{\sqrt{2}}\frac{1}{q_1^2}\frac{1}{u_1 - m_\eta^2} \times \left(\bar{v}(k_1)P_L v(p_2)\right)\left(\bar{u}(p_1)\gamma^\mu P_L \not{q}_1 u(k_2)\right)\epsilon_\mu^Q, \tag{5}$$

$$\mathcal{M}_c = -i\frac{f^2 g}{\sqrt{2}}\frac{1}{q_2^2}\frac{1}{t_2 - m_\eta^2} \times \left(\bar{v}(k_2)P_L \not{q}_2 \gamma^\mu v(p_2)\right)\left(\bar{u}(p_1)P_R u(k_1)\right)\epsilon_\mu^Q, \tag{6}$$

$$\mathcal{M}_d = -i\frac{f^2 g}{\sqrt{2}}\frac{1}{q_2^2}\frac{1}{u_2 - m_\eta^2} \times \left(\bar{v}(k_1)P_L \not{q}_2 \gamma^\mu v(p_2)\right)\left(\bar{u}(p_1)P_R u(k_2)\right)\epsilon_\mu^Q, \tag{7}$$

$$\mathcal{M}_e = -i\frac{f^2 g}{\sqrt{2}}\frac{1}{t_3 - m_\eta^2}\frac{1}{t_3' - m_\eta^2} \times \left(\bar{v}(k_2)P_L v(p_2)\right)\left(\bar{u}(p_1)P_R u(k_1)\right) \times \left((k_1 - p_1) + (k_1 - p_1 - Q)\right)^\mu \epsilon_\mu^Q, \tag{8}$$

$$\mathcal{M}_f = -i\frac{f^2 g}{\sqrt{2}}\frac{1}{u_3 - m_\eta^2}\frac{1}{u_3' - m_\eta^2} \times \left(\bar{v}(k_1)P_L v(p_2)\right)\left(\bar{u}(p_1)P_R u(k_2)\right) \times \left((k_2 - p_1) + (k_2 - p_1 - Q)\right)^\mu \epsilon_\mu^Q, \tag{9}$$

where we define the usual helicity projectors $P_{R/L} \equiv \frac{1}{2}(1 \pm \gamma_5)$, and the Mandelstam variables

$$\begin{aligned}
t_1 &= (k_1 - q_1)^2,\\
t_2 &= (k_1 - p_1)^2 = t_3,\\
u_1 &= (k_2 - q_1)^2,\\
u_2 &= (k_2 - p_1)^2 = u_3,\\
t_3' &= (k_2 - p_2)^2 = (k_1 - p_1 - Q)^2,\\
u_3' &= (k_1 - p_2)^2 = (k_2 - p_1 - Q)^2.
\end{aligned}$$

The vertex factors used in the matrix elements are as follows: the $l\nu W$ vertex has an $\frac{ig}{\sqrt{2}}\gamma^\mu P_L \epsilon_\mu^Q$, the $\chi\eta l$ vertex is $if P_L$, and the coupling between the W^- and the $\eta^+ - \eta^0$ is taken to be of the form $-ig(p + p')/\sqrt{2}$ from Ref. [21]. Fierz transformed versions of these matrix elements, and some insight gained from them, are collected in Appendix A.

We have explicitly checked the gauge invariance of our set of Feynman diagrams. Writing the matrix element as

$$\mathcal{M} = \mathcal{M}^\mu \epsilon_\mu^Q, \tag{10}$$

the Ward identity

$$Q_\mu \mathcal{M}^\mu = 0, \tag{11}$$

is satisfied for the sum of the diagrams. The Ward identity takes the same form as for photon bremsstrahlung provided we take the lepton masses to be zero, since the axial vector current is conserved in this limit. Note that diagrams (a) + (c) + (e) form a gauge-invariant subset, as do (b) + (d) + (f). The full amplitude is the sum of the partial amplitudes, properly weighted by a minus sign when two fermions are interchanged. Thus we have $\mathcal{M} = (\mathcal{M}_a + \mathcal{M}_c + \mathcal{M}_e) - (\mathcal{M}_b + \mathcal{M}_d + \mathcal{M}_f)$.

In performing the sum over spins and polarizations, we note the standard polarization sum,

$$\sum_{\text{pol.}} \epsilon_\mu^Q \epsilon_\nu^Q = -\left(g_{\mu\nu} - \frac{Q_\mu Q_\nu}{m_W^2}\right), \tag{12}$$

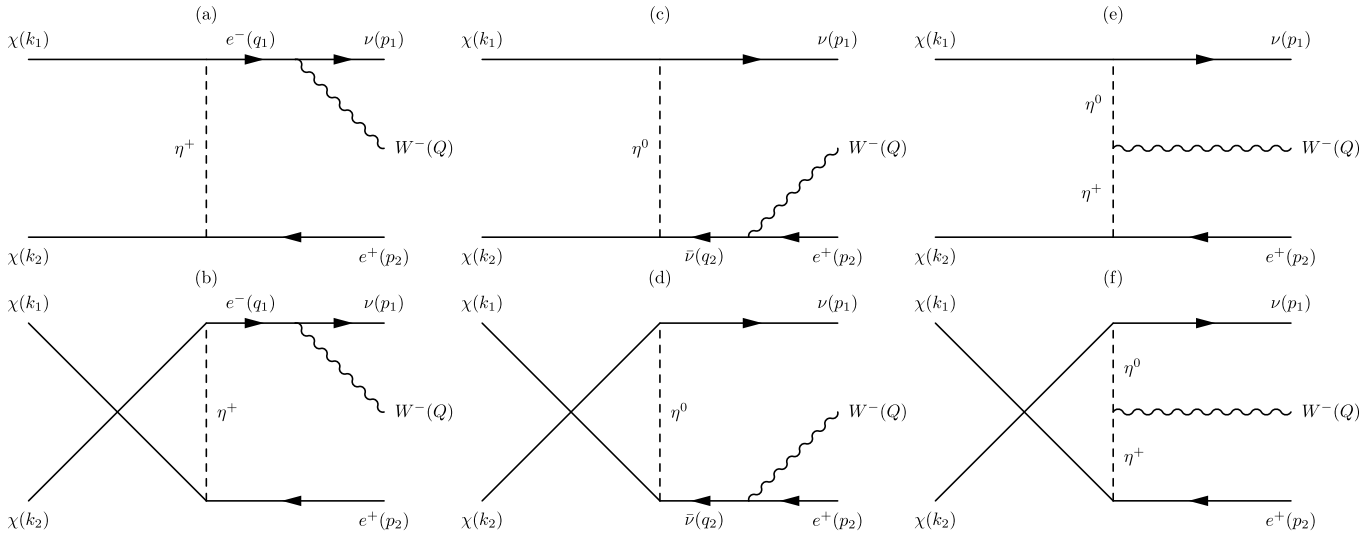

Fig. 1. The t-channel ((a), (c), and (e)) and u-channel ((b), (d) and (f)) Feynman diagrams for $\chi\chi \to e^+\nu W^-$. Note that t- and u-channel amplitudes are simply related by the $k_1 \leftrightarrow k_2$ interchange symmetry. All fermion momenta in the diagrams flow with the arrow except p_2 and q_2, with $q_1 = p_1 + Q$, $q_2 = p_2 + Q$.

can be replaced with $-g_{\mu\nu}$ alone. The Ward identity of Eq. (11) ensures the second term in Eq. (12) does not contribute once the contributions from all diagrams are summed (and squared).

In addition, we find that the longitudinal polarization of the W also does not contribute to the s-wave amplitude, i.e.

$$\mathcal{M}^{\mu}\epsilon^{Q}_{L\,\mu} = 0. \tag{13}$$

The W boson behaves as a massive transverse photon, with just two transverse polarizations contributing. As a consequence, our calculation of W bremsstrahlung must reduce to the known results for photon bremsstrahlung in the $m_W \to 0$ limit, modulo coupling constants. Below we will show that this happens.

The thermally-averaged cross section is given by

$$v\,d\sigma = \frac{1}{2s}\int \frac{1}{4}\sum_{\text{spin,pol.}} |\mathcal{M}|^2\, dLips^3 \tag{14}$$

where the $\frac{1}{4}$ arises from averaging over the spins of the initial χ pair, $v = \sqrt{1-\frac{4m_\chi^2}{s}}$ is the mean dark matter velocity, as well as the dark matter single-particle velocity in the center of mass frame,[2] and $dLips^n$ represents n-body Lorentz-invariant phase space.

We calculate the cross section for W emission following the procedure outlined above, with the integration over phase space performed according to the method described in Ref. [1]. We expand in powers of the DM velocity, v, keeping only the leading order (v^0) contribution. As expected, we have an unsuppressed cross section given by

$$\begin{aligned}
\sigma v \simeq \frac{\alpha_W f^4}{256\pi^2 m_\chi^2}\Bigg\{&(\mu+1)\Bigg[\frac{\pi^2}{6} - \ln^2\!\left(\frac{2m_\chi^2(\mu+1)}{4m_\chi^2\mu - m_W^2}\right)\\
&- 2\,\mathrm{Li}_2\!\left(\frac{2m_\chi^2(\mu+1)-m_W^2}{4m_\chi^2\mu - m_W^2}\right)\\
&+ 2\,\mathrm{Li}_2\!\left(\frac{m_W^2}{2m_\chi^2(\mu+1)}\right) - \mathrm{Li}_2\!\left(\frac{m_W^2}{m_\chi^2(\mu+1)^2}\right)\\
&- 2\,\mathrm{Li}_2\!\left(\frac{m_W^2(\mu-1)}{2(m_\chi^2(\mu+1)^2 - m_W^2)}\right)\\
&+ 2\ln\!\left(\frac{4m_\chi^2\mu - m_W^2}{2m_\chi^2(\mu-1)}\right)\ln\!\left(1 - \frac{m_W^2}{2m_\chi^2(\mu+1)}\right)\\
&+ \ln\!\left(\frac{m_W^2(\mu-1)^2}{4(m_\chi^2(\mu+1)^2 - m_W^2)}\right)\ln\!\left(1 - \frac{m_W^2}{m_\chi^2(\mu+1)^2}\right)\Bigg]\\
&+ \frac{(4\mu+3)}{(\mu+1)}\\
&- \frac{m_W^2(4m_\chi^2(\mu+1)(4\mu+3) - (m_W^2 - 4m_\chi^2)(\mu-3))}{16m_\chi^4(\mu+1)^2}\\
&+ \frac{m_W^2(4m_\chi^4(\mu+1)^4 - 2m_W^2m_\chi^2(\mu+1)(\mu+3) - m_W^4(\mu-1))}{4m_\chi^4(\mu+1)^3(m_\chi^2(\mu+1)^2 - m_W^2)}\\
&\times \ln\!\left(\frac{m_W^2}{4m_\chi^2}\right)\\
&+ \ln\!\left(\frac{2m_\chi^2(\mu-1)}{2m_\chi^2(\mu+1) - m_W^2}\right)\\
&\times \frac{(\mu-1)(2m_\chi^2(\mu+1) - m_W^2)}{4m_\chi^4(\mu+1)^3(4m_\chi^2\mu - m_W^2)(m_\chi^2(\mu+1)^2 - m_W^2)}\\
&\times \big(4m_\chi^6(\mu+1)^4(4\mu+1)\\
&- m_\chi^4 m_W^2(\mu+1)^2\big(3\mu(\mu+6)+7\big)\\
&+ 2m_\chi^2 m_W^4\big(\mu(\mu+4)+1\big) - m_W^6\big)\Bigg\}
\end{aligned} \tag{15}$$

where $\alpha_W \equiv g^2/(4\pi)$. The Spence function (or "dilogarithm") is defined as $\mathrm{Li}_2(z) \equiv -\int_0^z \frac{d\zeta}{\zeta}\ln|1-\zeta| = \sum_{k=1}^{\infty}\frac{z^k}{k^2}$.

If we take the limit $m_W \to 0$ and replace α_W with $2\alpha_{\text{em}}$, then Eq. (15) reproduces the cross section for bremsstrahlung of photons, namely[3]

[2] Informative discussions of the meaning of v are given in [22], and the inclusion of thermal averaging is covered in [23]. Note that we define v to be the dark matter single particle velocity in the center of mass frame, which in the non-relativistic limit is one-half of the (more commonly used) dark matter relative velocity.

[3] Note that Eq. (2) of Ref. [16] is larger by an overall factor of two, and also has the opposite sign for the $(1+\mu)[\ldots]$ term, while Eq. (1) of Ref. [16] is consistent with our results.

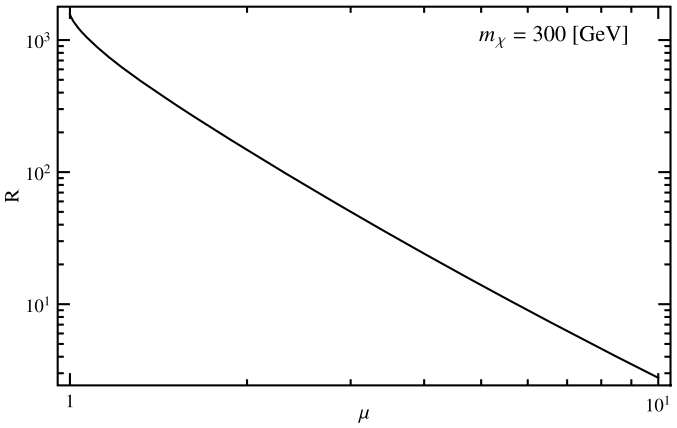

Fig. 2. The ratio $R = v\sigma(\chi\chi \to e^+\nu W^-)/v\sigma(\chi\chi \to e^+e^-)$ as a function of $\mu = (m_\eta/m_\chi)^2$, for $m_\chi = 300$ GeV. We have used $v = 10^{-3}c$, appropriate for the Galactic halo.

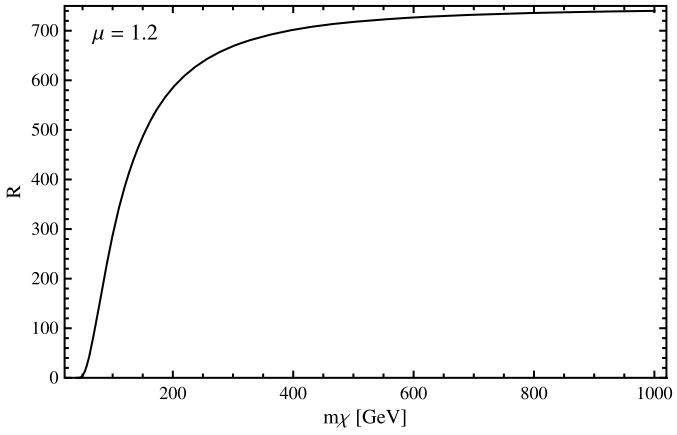

Fig. 3. The ratio $R = v\sigma(\chi\chi \to e^+\nu W^-)/v\sigma(\chi\chi \to e^+e^-)$ as a function of the DM mass m_χ, for $\mu = 1.2$ GeV. We have used $v = 10^{-3}c$, appropriate for the Galactic halo.

$$\sigma v \simeq \frac{\alpha_{\rm em} f^4}{128\pi^2 m_\chi^2}\left\{(\mu+1)\left[\frac{\pi^2}{6} - \ln^2\left(\frac{\mu+1}{2\mu}\right) - 2\,{\rm Li}_2\left(\frac{\mu+1}{2\mu}\right)\right] + \frac{4\mu+3}{\mu+1} + \frac{4\mu^2-3\mu-1}{2\mu}\ln\left(\frac{\mu-1}{\mu+1}\right)\right\}. \quad (16)$$

The successful recovery of the photon bremsstrahlung result in the massless W limit provides a check[4] on the rather complicated expression for massive W bremsstrahlung given above in Eq. (15).

Since we are working in the limits $v = 0$ and $m_f = 0$, the nonzero results in Eqs. (15) and (16) imply that the leading terms are neither helicity nor velocity suppressed. Not clear from the mathematical expressions is the sensible fact that the cross sections fall monotonically with increasing m_η (or μ). This monotonic fall is shown in Fig. 2, where we plot the ratio of the W-strahlung cross section to that of the lowest order process, $R = v\sigma(\chi\chi \to e^+\nu W^-)/v\sigma(\chi\chi \to e^+e^-)$. The lowest order process itself falls as μ^{-2}, so the W-strahlung process falls as μ^{-4}. This latter dependence is expected for processes with two propagators each off-shell by $1/\mu$, thereby signaling leading order cancellations among Fig. 1 diagrams (a)–(d).

[4] A related work [24] appeared on the arXiv nearly simultaneously with ours. In this related work there appears analytic expressions for the $M_Z, M_W = 0$ limits of the cross section which we calculate, thereby providing another calculational check.

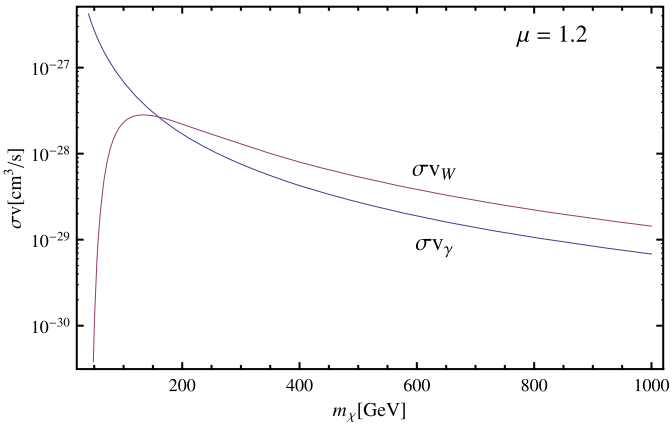

Fig. 4. The cross sections for $\chi\chi \to e^+\nu W^-$ (red) and $\chi\chi \to e^+e^-\gamma$ (blue), for $\mu = 1.2$ and coupling $f = 1$. For large DM mass, the cross sections differ by a factor of $1/(2\sin^2\theta_W) = 2.17$ while for m_χ comparable to m_W the W bremsstrahlung cross section is suppressed by phase space effects. (For interpretation of the references to color in this figure legend, the reader is referred to the web version of this Letter.)

Importantly, the effectiveness of the W-strahlung processes in lifting suppression of the annihilation rate is evident in Fig. 2. The ratio is maximized for μ close to 1, where m_χ and m_η are nearly degenerate. However, the W-strahlung process dominates over the tree level annihilation even if a mild hierarchy between m_χ and m_η is assumed. The ratio exceeds 100 for $\mu \lesssim 2$.

Fig. 3 illustrates that the ratio R is insensitive to the DM mass, except for low m_χ where the W mass significantly impacts phase space. From the figure one gleans that for $m_\chi \gtrsim 3m_W$, the ratio R is already near to its asymptotic value. Incidentally, the asymptotic value may be obtained analytically by dividing Eq. (16) with Eq. (3) and rescaling $\alpha_{\rm em}$ with $\alpha_W/2$.

In Fig. 4 we compare the W-strahlung cross section with that for photon bremsstrahlung. For high dark matter masses where the W mass is negligible, the two cross sections are identical except for the overall normalization, which is higher by factor of $1/(2\sin^2\theta_W) = 2.17$ for W-strahlung. For lower DM mass, the available phase space is reduced due to W mass effects, thus the W-strahlung cross section falls below that for photons. This can be seen in Fig. 4 for $m_\chi \lesssim 150$ GeV (this number is fairly insensitive to μ). Another factor of two is gained for W-strahlung when the W^+ mode is added to the W^- mode shown here.

Nominally, the correct dark matter energy fraction is obtained for early-Universe thermal decoupling with an annihilation cross section of 3×10^{-26} cm^3/s. It is seen in Fig. 4 that the W-strahlung mode falls 2–3 orders of magnitude below this value. Note that at the time of dark matter freeze-out in the early Universe, the velocity suppression of the p-wave contribution is not as severe as it is for late-Universe annihilation. Hence, radiative W-strahlung with its natural suppression factor $\alpha_W/4\pi$ is probably not the dominant annihilation mode responsible for early-Universe decoupling of Majorana dark matter.

3.2. W and lepton spectra

To obtain the energy spectrum of the W, we compute the differential cross section in terms of E_W by making the transformation

$$d\cos(\theta_q) \to \frac{-4\sqrt{s}q^2}{(s-q^2)(q^2-m_W^2)}\,dE_W. \quad (17)$$

The energy spectrum of the primary leptons is calculated in similar fashion. We find

$$
\begin{aligned}
v\frac{d\sigma}{dx_W} = {} & \frac{\alpha_W f^4}{128\pi^2 m_\chi^2}\left((1-x_W)+\frac{m_W^2}{4m_\chi^2}\right) \\
& \times\left\{\sqrt{x_W^2-\frac{m_W^2}{m_\chi^2}}\left[\frac{2}{\left((\mu+1)(\mu+1-2x_W)+\frac{m_W^2}{m_\chi^2}\right)}\right.\right. \\
& \left.\left.-\frac{1}{(\mu+1-x_W)^2}\right]\right. \\
& -\frac{\left((\mu+1)(\mu+1-2x_W)+\frac{m_W^2}{m_\chi^2}\right)}{2(\mu+1-x_W)^3} \\
& \left.\times\ln\left(\frac{\mu+1-x_W+\sqrt{x_W^2-m_W^2/m_\chi^2}}{\mu+1-x_W-\sqrt{x_W^2-m_W^2/m_\chi^2}}\right)\right\}, \qquad (18)
\end{aligned}
$$

$$
\begin{aligned}
v\frac{d\sigma}{dx_l} = {} & \frac{\alpha_W f^4}{512\pi^2 m_\chi^2}\frac{1}{(\mu-1+2x_l)^2} \\
& \times\left\{\left(4(1-x_l)^2-4x_l(\mu+1)+3(\mu+1)^2\right.\right. \\
& \left.-\frac{m_W^2}{m_\chi^2}(\mu+3)\right) \\
& \times\ln\left(\frac{2m_\chi^2(\mu+1)(1-x_l)-m_W^2}{(2m_\chi^2(\mu+1-2x_l)-m_W^2)(1-x_l)}\right) \\
& -\frac{x_l(4m_\chi^2(1-x_l)-m_W^2)}{(2m_\chi^2(1-x_l)(\mu+1)-m_W^2)(1-x_l)^2} \\
& \times\left[(1-x_l)^2\left(4(1-x_l)^2-x_l(\mu+1)+3(\mu+1)^2\right)\right. \\
& +\frac{m_W^2}{4m_\chi^2}(1-x_l)\left(x_l(\mu+11)-4(\mu+3)\right) \\
& \left.\left.-x_l\frac{m_W^2}{8m_\chi^2}\right]\right\}. \qquad (19)
\end{aligned}
$$

The W spectrum per $\chi\chi \to e\nu W$ event is given in Fig. 5. We use the scaling variable $x_W \equiv E_W/m_\chi$, and plot $dN/dx_W \equiv (\frac{1}{\sigma_{e^+\nu W^-}})\frac{d\sigma_{e^+\nu W^-}}{dx_W}$. The kinematic range of x_W is $[\frac{m_W}{m_\chi}, (1+\frac{m_W^2}{4m_\chi^2})]$, with the lower limit corresponding to a W produced at rest, and the upper limit corresponding to parallel lepton momenta balancing the opposite W momentum. As evident in Fig. 5, the W boson spectrum has a broad energy distribution, including a significant high energy component.

For the lepton energy spectrum, shown in Fig. 6, the range of the scaling variable $x_\ell \equiv E_\ell/m_\chi$ is $[0, 1-\frac{m_W^2}{4m_\chi^2}]$. Both limits arise when one lepton has zero energy and the other is produced back-to-back with the W. Note that this spectrum is valid for either the e^+ or the ν from the annihilation $\chi\chi \to e^+\nu W^-$, and for either e^- or $\bar{\nu}$ from the annihilation $\chi\chi \to e^-\bar{\nu}W^+$.

3.3. Z emission

Consider the process producing the $\bar{\nu}\nu Z$ final state. The cross sections for the Z-strahlung processes are related to those for W-strahlung in a simple way: The amplitudes producing $\bar{\nu}\nu Z$ arise from the same six graphs of Fig. 1, where e, W and η^+ are replaced everywhere by ν and Z and η_0, respectively. The calculation of the amplitudes, and their interferences, proceeds in an identical fashion. After making the replacement $m_W \to m_Z$, the cross section for the annihilation process $\chi\chi \to \nu\bar{\nu}Z$ differs from that for $\chi\chi \to e^+\nu W^-$ by only an overall normalization factor,

$$
\begin{aligned}
v\sigma_{\nu\bar{\nu}Z} &= \frac{1}{(2\cos^2\theta_W)} \times v\sigma_{e^+\nu W^-}\Big|_{m_W\to m_Z} \\
&\simeq 0.65 \times v\sigma_{e^+\nu W^-}|_{m_W\to m_Z}. \qquad (20)
\end{aligned}
$$

Consider now the e^+e^-Z final state. Again, the amplitudes arise from the same six basic graphs of Fig. 1. Since only the left-handed leptons couple to the dark matter via the $SU(2)$ doublet η, only the left-handed component of e^- participates in the interaction with the Z. Therefore, the couplings of the charged leptons to Z and W take the same form, up to a normalization constant. We thus find

$$
\begin{aligned}
v\sigma_{e^+e^-Z} &= \frac{2(\sin^2\theta_W-\frac{1}{2})^2}{\cos^2\theta_W} \times v\sigma_{e^+\nu W^-}\Big|_{m_W\to m_Z} \\
&\simeq 0.19 \times v\sigma_{e^+\nu W^-}|_{m_W\to m_Z}. \qquad (21)
\end{aligned}
$$

Adding the four contributions to W/Z-strahlung, we find

$$
v\sigma_{W/Z\text{-strahlung}} = 2.84 \times v\sigma_{e^+\nu W^-}. \qquad (22)
$$

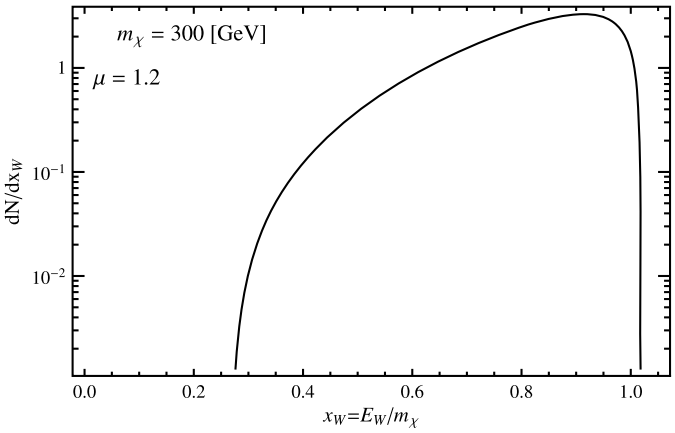

Fig. 5. The W spectrum per $\chi\chi \to e\nu W$ annihilation for $m_\chi = 300$ GeV and $\mu = 1.2$.

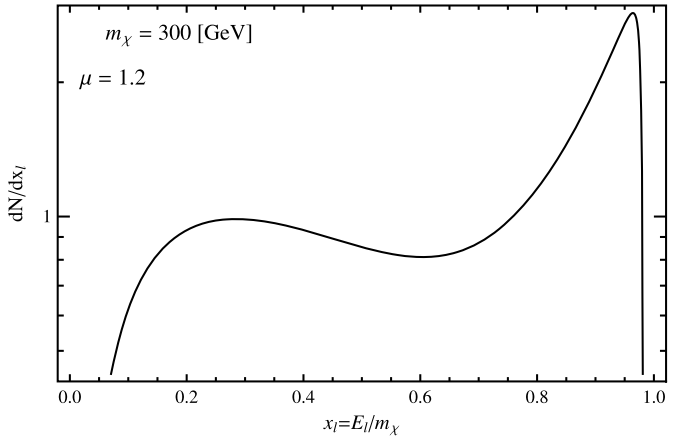

Fig. 6. The primary lepton spectrum per $\chi\chi \to e\nu W$ annihilation, for $m_\chi = 300$ GeV and $\mu = 1.2$.

4. Discussion and conclusions

There are clear advantages and disadvantages of seeking photon- versus W/Z-bremsstrahlung as an indirect signature of dark matter. With photon bremsstrahlung, the photon itself is

easily detected. It's energy spectrum may then be readily compared to model predictions. With W-strahlung, it is the decay products of the W decay which must be sought. Their spectra are less attributable to the model of dark matter annihilation. However, the total rate for W/Z-strahlung exceeds that of photon-strahlung. Photons couple with strength e, W's couple with strength $g/\sqrt{2} = e/(\sqrt{2}\sin\theta_W)$, and Z's couple to neutrinos with strength $g/(2\cos\theta_W) = e/(2\cos\theta_W \sin\theta_W)$. Therefore in the high energy limit where the W and Z masses can be neglected, we expect

$$\sigma_{e^+\nu W^-} = \frac{1}{2\sin^2\theta_W}\sigma_{e^+e^-\gamma} = 2.17\sigma_{e^+e^-\gamma}. \tag{23}$$

So, in the high energy limit where $m_\chi \gtrsim 300\ \text{GeV} \gg m_W$, the total cross section becomes

$$\begin{aligned}\sigma_{\text{brem,total}} &= \sigma_{e^+\nu W^-} + \sigma_{\bar\nu e^- W^+} + \sigma_{\bar\nu\nu Z} + \sigma_{e^+e^- Z} + \sigma_{e^+e^-\gamma} \\ &= 7.16\sigma_{e^+e^-\gamma}.\end{aligned} \tag{24}$$

Furthermore, the varied decay products of the W/Z allow more multi-messenger experiments to engage in the dark matter search. Charged leptons, protons and antiprotons, neutrinos, and even deuterons are expected, at calculable rates and with predictable spectra. Importantly, hadronic decay products are unavoidable, despite a purely leptonic tree-level annihilation. The tens of millions of Z events produced at CERN's e^+e^- collider show in detail what the branching fractions and spectra are for each kind of decay product. In a forthcoming article [9] we explore the favorable prospects for using W-strahlung decay products as indirect signatures for dark matter.

The lifting of the helicity suppression is most significant in the limit where the mass of the boson mediating dark matter annihilation does not greatly exceed the mass of the dark matter particle. This is true both for photon bremsstrahlung and for W/Z-bremsstrahlung. In this limit, we find the three body final state annihilation channels can significantly dominate over two body annihilation channels. The region of parameter space where χ and η are approximately degenerate is of great interest in many models, since it coincides with the co-annihilation region where both $\chi\chi$ and $\chi\eta$ annihilations are important in determining the relic dark matter density at the time of freezeout in the early Universe, often a favored parameter region in SUSY scenarios.

Acknowledgements

We thank Paolo Ciafaloni, Alfredo Urbano, and Ray Volkas for helpful discussions. J.B.D. was supported in part by the Arizona State University Cosmology Initiative, L.M.K. was supported by the US Department of Energy, N.F.B. was supported by the Australian Research Council, A.J.G. and T.D.J. were supported by the Commonwealth of Australia, and T.J.W. was supported in part by U.S. DoE grant DE-FG05-85ER40226.

Appendix A. Fierz transformed matrix elements

Upon Fierz transforming (for standard $2 \to 2$ Fierz identities, see e.g., [25,26]) the matrix elements of Eqs. (4)–(9) we find

$$\begin{aligned}\mathcal{M}_a &= \frac{igf^2}{\sqrt{2}q_1^2}\frac{1}{t_1 - m_\eta^2}\frac{1}{2}\big(\bar v(k_2)\gamma_\alpha P_R u(k_1)\big) \\ &\quad\times\big(\bar u(p_1)\gamma^\mu \not q_1 \gamma^\alpha P_L v(p_2)\big)\epsilon_\mu^Q,\end{aligned} \tag{A.1}$$

$$\begin{aligned}\mathcal{M}_b &= \frac{igf^2}{\sqrt{2}q_1^2}\frac{1}{u_1 - m_\eta^2}\frac{1}{2}\big(\bar v(k_2)\gamma_\alpha P_L u(k_1)\big) \\ &\quad\times\big(\bar u(p_1)\gamma^\mu \not q_1 \gamma^\alpha P_L v(p_2)\big)\epsilon_\mu^Q,\end{aligned} \tag{A.2}$$

$$\begin{aligned}\mathcal{M}_c &= \frac{-igf^2}{\sqrt{2}q_2^2}\frac{1}{t_2 - m_\eta^2}\frac{1}{2}\big(\bar v(k_2)\gamma_\alpha P_R u(k_1)\big) \\ &\quad\times\big(\bar u(p_1)\gamma^\alpha \not q_2 \gamma^\mu P_L v(p_2)\big)\epsilon_\mu^Q,\end{aligned} \tag{A.3}$$

$$\begin{aligned}\mathcal{M}_d &= \frac{-igf^2}{\sqrt{2}q_2^2}\frac{1}{u_2 - m_\eta^2}\frac{1}{2}\big(\bar v(k_2)\gamma_\alpha P_L u(k_1)\big) \\ &\quad\times\big(\bar u(p_1)\gamma^\alpha \not q_2 \gamma^\mu P_L v(p_2)\big)\epsilon_\mu^Q,\end{aligned} \tag{A.4}$$

$$\begin{aligned}\mathcal{M}_e &= \frac{-igf^2}{2\sqrt{2}}\frac{(2k_1 - 2p_1 - Q)^\mu}{(t_3' - m_\eta^2)(t_3 - m_\eta^2)}\big(\bar v(k_2)\gamma_\alpha P_R u(k_1)\big) \\ &\quad\times\big(\bar u(p_1)\gamma^\alpha P_L v(p_2)\big)\epsilon_\mu^Q,\end{aligned} \tag{A.5}$$

$$\begin{aligned}\mathcal{M}_f &= \frac{-igf^2}{2\sqrt{2}}\frac{(2k_2 - 2p_1 - Q)^\mu}{(u_3' - m_\eta^2)(u_3 - m_\eta^2)}\big(\bar v(k_2)\gamma_\alpha P_L u(k_1)\big) \\ &\quad\times\big(\bar u(p_1)\gamma^\alpha P_L v(p_2)\big)\epsilon_\mu^Q.\end{aligned} \tag{A.6}$$

Alternatively, we may apply a chiral version of the Fierz transform (discussed in detail in Ref. [1].) to transform Eqs. (4)–(9). After a bit of algebra we get a pleasant factorized form for the bilinear currents. We show details for the first one, and then summarize the results for current products of the other matrix elements.

The current product in amplitude M_a of Eq. (4) is

$$\big(\bar v(k_2)P_L v(p_2)\big)\big(\bar u(p_1)\not\epsilon^Q P_L \not q_1 u(k_1)\big). \tag{A.7}$$

We write this current product in Takahashi notation [26] and then use the chiral Fierz transform to obtain

$$\begin{aligned}[P_L](\not\epsilon^Q P_L \not q_1) &= \frac{1}{4}\operatorname{Tr}[P_L \Gamma^C \not\epsilon^Q P_L \not q_1 \Gamma_B](\Gamma^B][\Gamma_C) \\ &= \frac{1}{4}\operatorname{Tr}[P_L\gamma^\alpha \not\epsilon^Q P_L \not q_1 \gamma_\beta](P_R\gamma^\beta][P_L\gamma_\alpha).\end{aligned} \tag{A.8}$$

In going from the first equality to the second, we insert the only values for Γ^C and Γ_B allowed by the helicity projectors in the string of gamma matrices. Finally, we may invert the sequence in the trace, and remove the Takahashi notation to write the result as

$$\begin{aligned}&\frac{1}{4}\operatorname{Tr}[P_R \not\epsilon^Q P_L \not q_1 \gamma_\beta \gamma^\alpha] \\ &\quad\times\big(\bar u(p_1)P_R\gamma^\beta v(p_2)\big)\big(\bar v(k_2)P_L\gamma_\alpha u(k_1)\big).\end{aligned} \tag{A.9}$$

Amplitude M_b is computed in a similar way. In addition, it is useful to use the identity for a Majorana current

$$\big(\bar v(k_1)P_L\gamma_\alpha u(k_2)\big) = \big(\bar v(k_2)P_R\gamma_\alpha u(k_1)\big) \quad \text{[Majorana]} \tag{A.10}$$

to put the final result in a form similar to that for amplitude M_a. The other current products are reduced in a similar fashion. The final result for the product of currents after Fierzing is

$$\begin{aligned}&\frac{1}{4}\big(\bar v(k_2)P\gamma^\alpha u(k_1)\big)\big(\bar u(p_1)P_R\gamma^\beta v(p_2)\big) \\ &\quad\times\begin{cases}\operatorname{Tr}[P_R \not\epsilon^Q \not q_1 \gamma_\beta\gamma_\alpha], & \text{for } M_a,\ M_b, \\ \operatorname{Tr}[P_L \not\epsilon^Q \not q_2 \gamma_\beta\gamma_\alpha], & \text{for } M_c, M_d, \\ 2g_{\alpha\beta}, & \text{for } M_e, M_f.\end{cases}\end{aligned} \tag{A.11}$$

In addition, the unspecified projector P in the first common factor is P_L for amplitudes M_a, M_c, M_e, and P_R for the amplitudes M_b, M_d, M_f derived from the crossed graphs.

What can we learn from this exercise? For graphs M_e and M_f the Fierzed currents are the same as in the $2 \to 2$ case. This fact is not surprising since in these graphs the internal W emission does not perturb the form of the currents and their product. However, for the other four graphs with W emission occurring on a fermion leg, the form of the current product is quite different

from the $2 \to 2$ case. With $2 \to 3$ scattering, the Lorentz index of each current need not contract directly with the other. Referring to Table 1 of Ref. [1], one sees that unsuppressed Majorana annihilation amplitudes become possible for the axial vector combination $(\gamma_5\gamma^0)[\gamma_5\vec{\gamma}_T)$, and for the vector combination $(\gamma^3][\vec{\gamma}_T)$, providing the trace post-factors in Eq. (A.11) do not vanish. These combinations are at the heart of the unsuppression which we have presented in this Letter. (The role of amplitudes M_e and M_f is to cancel gauge non-invariant contributions from graphs M_a–M_d.) See also Ref. [27] for a comprehensive discussion of enhanced/suppressed DM annihilation modes.

Also, for $m_\eta^2 \gg t, u$, the non-current factors in amplitudes M_a and M_b are the same, as are the non-current factors in amplitudes M_c and M_d. Then the subtraction of one from the other leads to a pure axial vector coupling in the Majorana current. This in term leads to an effectively pure axial vector coupling in the final state lepton current. This effective axial vector–axial vector coupling of currents was advertised earlier. However, for values of t and u which are non-negligible when compared to m_η^2, there is some residual vector coupling. In this more complicated case, it is probably best to directly calculate rates without Fierzing the currents. Such is the course followed in the main text of this Letter.

References

[1] N.F. Bell, J.B. Dent, T.D. Jacques, T.J. Weiler, Phys. Rev. D 83 (2011) 013001, arXiv:1009.2584 [hep-ph].
[2] V. Berezinsky, M. Kachelriess, S. Ostapchenko, Phys. Rev. Lett. 89 (2002) 171802, arXiv:hep-ph/0205218.
[3] M. Kachelriess, P.D. Serpico, Phys. Rev. D 76 (2007) 063516, arXiv:0707.0209 [hep-ph].
[4] N.F. Bell, J.B. Dent, T.D. Jacques, T.J. Weiler, Phys. Rev. D 78 (2008) 083540, arXiv:0805.3423.
[5] J.B. Dent, R.J. Scherrer, T.J. Weiler, Phys. Rev. D 78 (2008) 063509, arXiv:0806.0370 [astro-ph].
[6] M. Kachelriess, P.D. Serpico, M.A. Solberg, Phys. Rev. D 80 (2009) 123533, arXiv:0911.0001 [hep-ph].
[7] P. Ciafaloni, A. Urbano, Phys. Rev. D 82 (2010) 043512, arXiv:1001.3950 [hep-ph].
[8] P. Ciafaloni, D. Comelli, A. Riotto, F. Sala, A. Strumia, A. Urbano, JCAP 1103 (2011) 019, arXiv:1009.0224 [hep-ph].
[9] N.F. Bell, J.B. Dent, T.D. Jacques, T.J. Weiler, Phys. Rev. D (2011), in press, arXiv:1101.3357 [hep-ph].
[10] Massive three body final states were considered in X.l. Chen, M. Kamionkowski, JHEP 9807 (1998) 001.
[11] L.B. Okun, Leptons and Quarks, North-Holland, Amsterdam, The Netherlands, 1982, 361 p., Section 29.3.5.
[12] L. Bergstrom, Phys. Lett. B 225 (1989) 372.
[13] R. Flores, K.A. Olive, S. Rudaz, Phys. Lett. B 232 (1989) 377.
[14] E.A. Baltz, L. Bergstrom, Phys. Rev. D 67 (2003) 043516, arXiv:hep-ph/0211325.
[15] T. Bringmann, L. Bergstrom, J. Edsjo, JHEP 0801 (2008) 049, arXiv:0710.3169 [hep-ph].
[16] L. Bergstrom, T. Bringmann, J. Edsjo, Phys. Rev. D 78 (2008) 103520, arXiv:0808.3725 [astro-ph].
[17] V. Barger, Y. Gao, W.Y. Keung, D. Marfatia, Phys. Rev. D 80 (2009) 063537, arXiv:0906.3009 [hep-ph].
[18] Q.H. Cao, E. Ma, G. Shaughnessy, Phys. Lett. B 673 (2009) 152, arXiv:0901.1334 [hep-ph].
[19] E. Ma, Phys. Rev. Lett. 86 (2001) 2502, arXiv:hep-ph/0011121.
[20] H. Goldberg, Phys. Rev. Lett. 50 (1983) 1419;
Making use of some earlier Fierzing by P. Fayet, Phys. Lett. B 86 (1979) 272;
See L.M. Krauss, Nucl. Phys. B 227 (1983) 556, for cosmological implications.
[21] H.E. Haber, G.L. Kane, Phys. Rept. 117 (1985) 75, see Fig. 72b on p. 221 of Appendix C.
[22] L.D. Landau, E.M. Lifschitz, The Classical Theory of Fields, 4th revised English edition, Pergamon Press, 1975, pp. 32–34.
[23] P. Gondolo, G. Gelmini, Nucl. Phys. B 360 (1991) 145.
[24] P. Ciafaloni, M. Cirelli, D. Comelli, A. De Simone, A. Riotto, A. Urbano, JCAP 1106 (2011) 018, arXiv:1104.2996 [hep-ph].
[25] C. Itzykson, J.B. Zuber, Quantum Field Theory, Dover Press, 1980, pp. 161–162; C.C. Nishi, Am. J. Phys. 73 (2005) 1160, arXiv:hep-ph/0412245.
[26] Y. Takahashi, The Fierz identities, in: H. Ezawa, S. Kamefuchi (Eds.), Progress in Quantum Field Theory, North Holland, Amsterdam, 1986, p. 121.
[27] M. Lindner, A. Merle, V. Niro, arXiv:1005.3116 [hep-ph].